Biomaterials Science

COMMUNICATION

View Article Online
View Journal | View Issue

Cite this: *Biomater. Sci.*, 2017, **5**, 2398

Received 26th July 2017,
Accepted 30th September 2017

DOI: 10.1039/c7bm00669a

rsc.li/biomaterials-science

Degradable and biocompatible hydrogels bearing a hindered urea bond†

Hanze Ying, ‡[a] Jonathan Yen,‡§[b] Ruibo Wang,[a] Yang Lai,[c] Jer-Luen-Aaron Hsu,[a] Yuhang Hu*[c] and Jianjun Cheng *[a]

A hindered urea bond (HUB), recently reported as a new type of dynamic chemical bond, can be facilely constructed by mixing an isocyanate and a hindered amine. Here, we report the use of the HUB in the design of degradable hydrogel materials for applications of stem cell encapsulation and delivery. Polyethyleneglycol (PEG) diamine was end-capped with a HUB and an allyl group in a one-pot synthesis. The resulting polymer was cross-linked to form a hydrogel under UV with the addition of a 4-arm PEG thiol and a photoinitiator. The degradation properties of the hydrogels were confirmed with NMR, GPC, weight loss, and protein release studies. We found that the degradation kinetics is dependent on the size of the *N*-substituents, and the one with the *tert*-butyl group shows complete degradation within 2 days. The new hydrogel materials were also demonstrated to be biocompatible with hMSCs, and the cell release kinetics can be facilely tuned over 5 days.

In the field of biomedical engineering, hydrogels have played integral roles in both tissue engineering and drug delivery applications.[1–10] Cellular encapsulation and growth in scaffolds are important aspects for tissue engineering. It is ideal to replace or supplement damaged or diseased tissue with *in vitro* engineered cells. But replacing the cells requires a suitable scaffold with various important properties.[2,9–11] The scaffolds need to be biocompatible, able to support cellular growth, and biodegradable. They should allow for structural support and nutrients to flow in and out to support the cells.[12–14] Many scaffolds have been developed to support the 3D culture for cellular therapies.[1,9,15,16] Hydrogels have proven to be one of the most ideal systems, which are usually composed largely of water held together with 1–20% of polymers formed together *via* covalent or noncovalent crosslinks.[17,18] The high water retention of these hydrogels allows for simple static mimetics of tissue environments. Their stiffness is also easily tunable from a few hundred Pa to a few kPa by tuning the polymeric compositions and ratios, allowing the support for various cell types for soft or hard tissues.[19–22]

Traditional hydrogels are stable and static due to the polymer type and covalent crosslinking. But these static hydrogels are missing key features that can hinder their applications for tissue engineering. These hydrogels can restrict the cellular movement, interaction with the environment, production of an extracellular matrix (ECM), and thus proper tissue repair and development.[23] The ideal hydrogel would need to be degradable to allow the cells to reorganize themselves and build a new ECM to restructure themselves into the desired tissue.[24] Many of the traditional hydrogels are naturally degradable *via* hydrolysis, but the degradation can take weeks or even months, much too long for any cellular restructuring. In the past few years, there have been many developments in degradable hydrogel systems that are triggerable *via* light,[25,26] temperature,[27,28] enzymes,[23,29,30] or pH.[31] But these systems require specific triggers that can be complex to incorporate into the backbone of the monomers and they may not be suitable nor can be found at the site of interest, thus a hydrogel that can be degraded naturally over a set amount of time is highly desirable.

A hindered urea bond (HUB), a urea structure containing a bulky substituent on one of the nitrogen atoms, was recently found to be hydrolyzable.[32–34] The HUB can naturally degrade in the presence of water at body temperature without any external triggers. Also, HUB structures can be quickly and efficiently constructed through simple mixing of an isocyanate and a secondary hindered amine, and their hydrolysis kinetics can be tuned from days to years through control of the bulkiness of the substituents, which makes them potential candidates for the design of hydrogel biomaterials. Previously we have demonstrated that hydrophilic cross-linked polymers containing HUBs can be completely degraded in water. However, the

[a]*Department of Materials Science and Engineering, University of Illinois at Urbana–Champaign, Urbana, IL, 61801, USA. E-mail: jianjunc@illinois.edu*
[b]*Department of Bioengineering, University of Illinois at Urbana–Champaign, Urbana, IL, 61801, USA*
[c]*Department of Mechanical Science and Engineering, University of Illinois at Urbana–Champaign, Urbana, IL, 61801, USA. E-mail: yuhanghu@illinois.edu*
†Electronic supplementary information (ESI) available. See DOI: 10.1039/c7bm00669a
‡These authors contributed equally.
§Current address: Chemical Biology and Therapeutics, Novartis Institutes for BioMedical Research, Cambridge, Massachusetts, 02139, USA.

preparation of hydrogels involves the use of small molecular methacrylate monomers, which are toxic to cells. Herein, we make a further step to explore the potential of HUB hydrogels for biomedical engineering applications. We report the design and synthesis of hydrophilic polymeric precursors containing HUB structures that can safely mix with cells, cross-link to hydrogel materials, and show fast hydrolysis kinetics and good biocompatibility with human mesenchymal stem cells.

The preparation of HUB hydrogels is based on a thiol–ene reaction between linear polyethylene glycol (PEG) bearing HUB groups end-capped by a double bond and 4-arm PEG end-capped by thiol groups (Scheme 1). The HUB bearing PEG precursors were synthesized through end-functionalization of commercially available PEG derivatives. Amine di-functional PEG (PEG-DA, $M_n \sim 2$ K) reacted with excess *m*-xylylene diisocyanate, which converted end groups to isocyanates. Without purification, *N*-substituted allylamine was directly added into the mixture to convert all isocyanate groups (including the ones in polymers and excess small molecules) into urea bonds. After that, the polymers were purified through precipitation with ethyl ether, while di-urea small molecules still remained intact in solution and were removed (see the synthetic scheme in Fig. 1a). Two types of *N*-substituted allylamine were used in the synthesis, one with a *tert*-butyl group (to create more bulky *tert*-butyl urea (TBU)) and the other with a methyl group (to create less bulky methyl urea (MU)). Fig. 1b shows the ^{1}H NMR characterization of these two polymers. The peaks from end groups (urea and allyl groups) can be clearly identified and well assigned to the designed structures. It is important to notice that the addition sequence of the first step has a big influence on the structure of the final product. Since the reaction between an isocyanate and an amine is very fast, one should add PEG-DA slowly into excess diisocyanate with vigorous stirring to reduce the chance of inter-chain coupling. In our experiment, some coupling products (dimer, trimer, *etc.*) were still observed in GPC, but the ratio is lower than 20% for both *tert*-butyl urea capped PEG (PEG-DTBU) and methyl urea capped PEG (PEG-DMU). However, when the addition sequence was reversed, the resulting polymer showed a much larger molecular weight and very low signal for end-capped double bonds due to the occurrence of many inter-chain couplings (Fig. S1 and 2†).

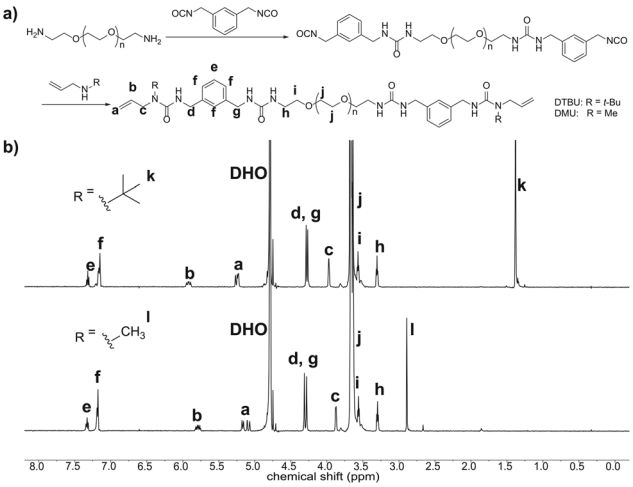

Fig. 1 Synthesis of HUB bearing polyethylene glycol precursors. (a) Two-step synthetic route of polyethylene glycol end-capped with HUB linkages and double bonds for thiol–ene crosslinking; (b) ^{1}H NMR spectra of PEG-DTBU and PEG-DMU in D_2O. Peaks were assigned to protons on chemical structures shown in (a).

Next we studied the hydrolysis of the HUB in PEG precursors. Based on the previous studies about the HUB hydrolysis mechanism,[33] we used the release rate of *N*-substituted allylamine to characterize the hydrolysis kinetics of the HUB (Fig. 2a). Two types of polymers, PEG-DTBU and PEG-DMU, were dissolved in deuterated water, and the production rate of *N*-substituted allylamine was monitored by ^{1}H NMR. As shown in Fig. 2b for PEG-DTBU with a more bulky HUB, the intensities of peaks a–c corresponding to the end *N*-*tert*-butyl allylamine groups decreased over time. However, new peaks a′–c′ next to their original peaks appeared and increased gradually, which were assigned to the released small molecules (Fig. 2b). The concentration of the released amine increased quasi-linearly with the rate of approximately 11% per day (Fig. 2c). However, for PEG-DMU with less bulky urea, no change in ^{1}H NMR was observed even after 130 h (Fig. 2c). This concluded that the hydrolysis behavior is related to the bulkiness of the HUB structure. We then used GPC to characterize the change in molecular size after water incubation for 2 days. After water degradation, the end group becomes amine, and may or may not couple with the released isocyanate from other chains to form a permanent urea bond (Fig. 2a). The coupling reaction doubles the molecular weight of the polymer. As shown in Fig. 2d, the GPC curves of PEG-DMU remained the same after incubation of 48 h showing no hydrolysis. In contrast, we observed the appearance of peaks for coupled chains for PEG-DTBU, which demonstrated that the end group has been hydrolyzed (Fig. 2d).

To synthesize HUB hydrogels, two PEG-HUB precursors were mixed with 4-arm PEG thiols (same equivalence of functional groups, 10% water solution) and UV cured through

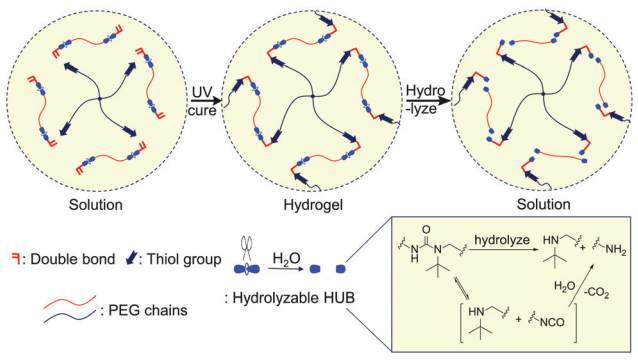

Scheme 1 Schematic illustration of the synthesis and degradation of hydrogel structures based on a hydrolysable hindered urea bond (HUB).

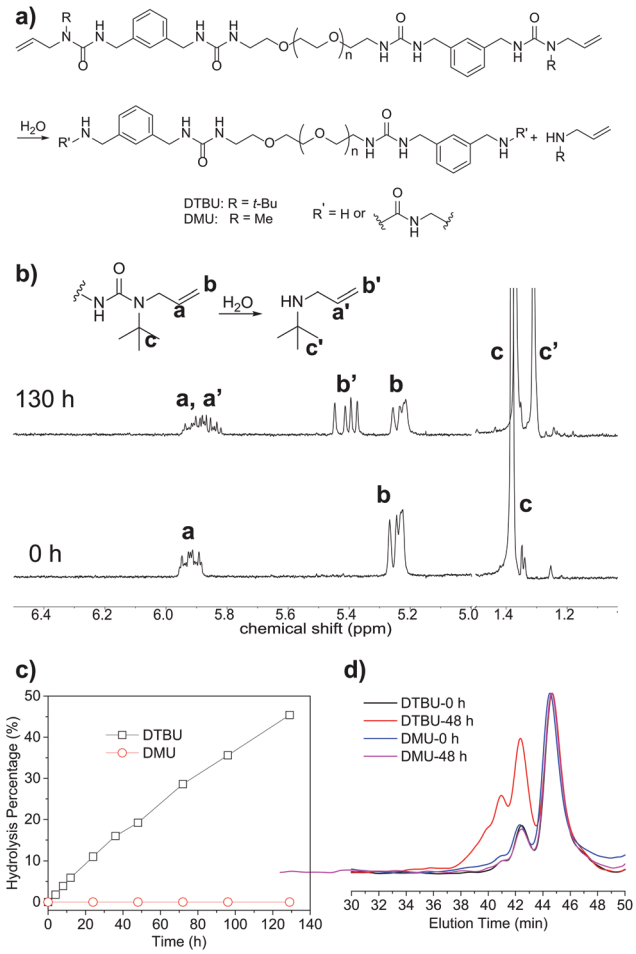

Fig. 2 Water degradation of a HUB in PEG-HUB precursors. (a) Degradation reaction of HUB structures at the end of the chain; (b) time dependent ^{1}H NMR spectra in D_2O showing new peaks of released amine over time; (c) plot of hydrolyzed HUB ratio *vs.* incubation time at 37 °C; (d) GPC curves of PEG-HUB before and after 48 h incubation in PBS solution.

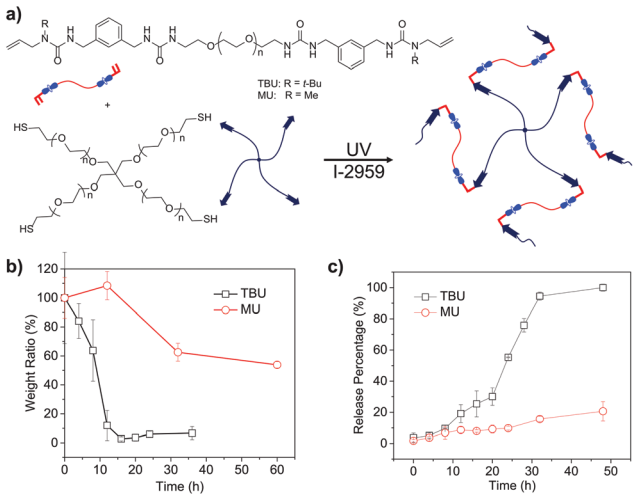

Fig. 3 Water degradation studies of HUB hydrogels. (a) Synthesis of HUB hydrogel through thiol–ene reaction. Four-arm PEG-thiol was used as a cross-linker; (b) weight change in TBU (black curve) and MU (red curve) after immersing in PBS for varying times; (c) release profile of BSA-FITC from HUB hydrogels over time. Data for both (b) and (c) represent averages of triplicate experiments. Error bars are standard deviation (n = 3).

thiol–ene reaction (Fig. 3a). The shear modulus of the TBU gel and the MU gel was measured through indentation tests by using an atomic force microscope (see ESI and Fig. S3† for experimental details). A spherical indenter was pressed into the samples and the force on the indenter was recorded as a function of indentation depth. Both the samples and the probes were kept in DI water during tests. The hydrogel is assumed to be incompressible. Through Hertzian contact solution, we can obtain the shear modulus of the sample, which is 10.0 ± 0.9 kPa for the TBU gel, and 4.7 ± 0.6 kPa for the MU gel. The error bar is for 8–10 measurements at different locations on each sample. Then the two gels were immersed into phosphate buffered saline (PBS) and the weight change was monitored at varying times with the incubation at 37 °C (gels were pre-treated with deionized water for 12 h). TBU based gels completely disappeared after 16 h. In contrast, MU based gel remained intact after 3 days (Fig. 3b). We noticed that the gel degradation speed for TBU seems higher than bond hydrolysis kinetics determined by ^{1}H NMR (20 h degradation time corresponding to ~10% bond breakage). It may be caused by the hydrolysis kinetic difference between normal water and deuterated water. The allyl group, which exists in the precursor but not in the final network, was also found to slow down the hydrolysis kinetics. Network defects, such as loops and unreacted monomers (the reason why MU gel also showed some weight loss), also reduce the amount of bond breakage needed for complete gel collapse.

For the potential applications of protein delivery, we encapsulated bovine serum albumin-fluorescein (BSA-Fluo) into the hydrogel and monitored the release of protein in PBS buffer overtime. TBU based gel released the protein gradually with the gel itself dissolved into aqueous solution. After 32 h, the whole piece of hydrogel disappeared and 100% of the dye was released. For non-degradable MU based gel, it still remained intact after the same time, and only less than 20% of the dye released out due to diffusion (Fig. 3c).

Human mesenchymal stem cells (hMSCs) are a widely used cell line for various tissue engineering applications for bone or cartilage repair. Thus, we tested the biocompatibility of the TBU hydrogel with hMSCs. Firstly, hMSCs were incubated with various concentrations of the HUB-PEG precursors for 48 h (Fig. 4a). After 48 h, an XTT assay was performed on the cells, in which they demonstrated over 100% viability in relation to untreated cells. hMSCs were then encapsulated in the TBEU hydrogel with varying concentrations of PEG-TBU. After 48 h encapsulation of the hMSCs within the hydrogel, XTT was conducted on the cells. In relation to an equivalent number of cells plated in 2D, the 5%, 10%, and 20% hydrogels demonstrated roughly 100% cell viability (Fig. 4b), indicating

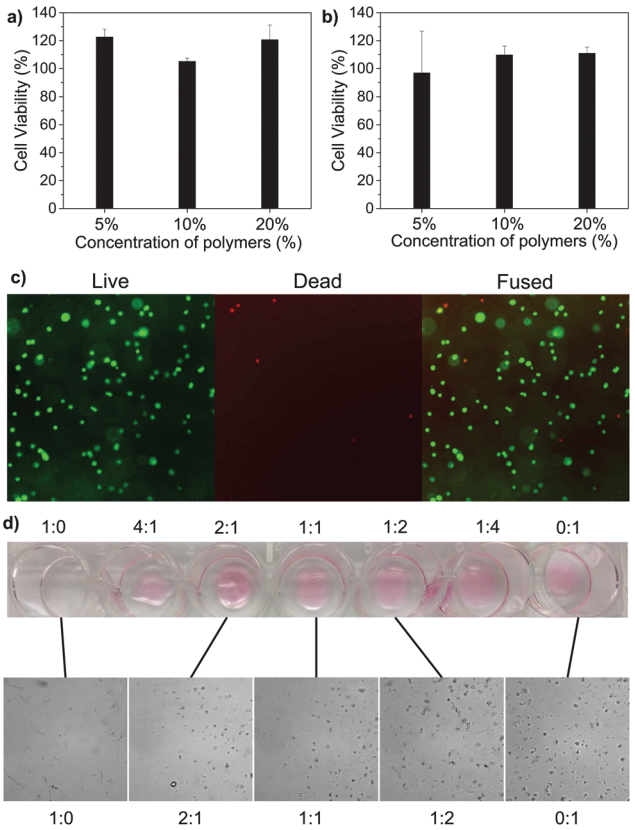

Fig. 4 Biocompatibility of TBEU hydrogel to human mesenchymal stem cells (hMSCs). (a) Cell viability after incubating hMSCs with HUB-PEG precursors for 48 h; (b) cell viability after encapsulating hMSCs in HUB-PEG hydrogels for 48 h. (c) Fluorescence live dead imaging of hMSCs encapsulated in TBEU/HUB-PEG hydrogels 48 h after encapsulation using a GE InCell Analyzer 2000. Green fluorescence indicates live cells and red staining indicates dead cells. Image analysis indicates 94% live cells. (d) hMSCs release from a degrading mixed backbone of TBEU : MEU hydrogel. The hydrogel was formed through thiol–ene UV crosslinking with hMSCs encapsulated inside. After 5 days culture of the hydrogel on tissue culture treated plates, all cells or part of cells escaped and adhered to the plate. The hydrogels and the plates were imaged. At 1 : 0 ratio the hydrogel was completely degraded and all the cells were released and adhered to the cells, while as the amount of MEU increases, the amount of hMSCs being released decreased significantly and more cells remained encapsulated.

the good biocompatibility of the hydrogel with hMSCs. Live/dead staining was also done to determine cell survival. The cells were imaged using a GE InCell analyzer, with multiple fields and *z* stack which were then collapsed into one focal plane for analysis. There is a survival rate of 94%. The high survivability indicates the excellent biocompatibility of the polymer and hydrogel to the hMSCs (Fig. 4c). Due to the rapid degradation of the PEG-TBEU backbone, the degradable PEG-TBEU was mixed with PEG-MEU to create a slow degrading and pore forming hydrogel for mobile stem cell encapsulation. PEG-TBEU was mixed with PEG-MEU at varying ratios at 1 : 0, 4 : 1, 2 : 1, 1 : 1 1 : 2, 1 : 4, and 0 : 1 with the encapsulation of hMSCs. After 5 days, the hydrogel and cells that were released and adhered to the plate were imaged. As expected at a 1 : 0 ratio of the TBEU : MEU backbone, the hydrogel was completely degraded and all the cells were released and adhered onto the plate. With the addition of the non-degradable MEU polymer, the hydrogel remained intact after 5 days. For the ratios of 4 : 1 and 2 : 1 of TBEU : MEU, although the hydrogels still remained intact, the hMSCs were able to migrate out from the gel and adhered to the plate. As we further increased the MEU ratio to 1 : 1, less cells were released and adhered to the plate and most cells remained encapsulated within the hydrogel. At 1 : 2, 1 : 4, and 0 : 1 ratios, we saw no release at all and all the cells remained encapsulated within the hydrogel, which could be seen in the images as the round non-adhered cells (Fig. 4d). It is clear that through the tuning of the ratios between degradable/non-degradable backbones in the hydrogels, the cell release profile can be well tuned. This biocompatible hydrogel system is promising for further studies such as increased pore formation, cell migration, cell restructuring, organogenesis, or cell delivery applications.

In summary, we for the first time demonstrated the use of a HUB, a trigger-free and fast hydrolyzing chemical bond, in the applications of hydrogel materials for stem cell encapsulations and delivery. Syntheses of HUB-containing, vinyl end-capped and non-toxic PEG precursors were developed, which can crosslink with multi-arm PEG thiols to form hydrogels. TBEU containing hydrogels were proved to completely degrade and efficiently release protein cargos within two days at 37 °C. This new TBEU containing hydrogel was shown to be non-cytotoxic and biocompatible with hMSCs. It has also proven to be quite tunable in the cell release kinetics over 5 days, in which we can control the amount of cells released back onto the plate over time. This TBEU hydrogel can be applied in the future for tissue engineering applications that require highly tunable and different release kinetics of cells or proteins to wound sites. In addition, due to the dynamic crosslinking of TBEU hydrogels, future applications with self-stiffening or self-relaxing hydrogels are being explored as well, thus altering the microenvironmental cues to encapsulated cells.

Author contributions

The manuscript was written through contributions of all authors. All authors have given approval to the final version of the manuscript.

Conflicts of interest

The authors declare no competing financial interest.

Acknowledgements

This work is supported by the United States National Science Foundation (CHENSF CHE 15-08710).

References

1 L. Bian, M. Guvendiren, R. L. Mauck and J. A. Burdick, *Proc. Natl. Acad. Sci. U. S. A.*, 2013, **110**, 10117–10122.
2 C. Borselli, C. A. Cezar, D. Shvartsman, H. H. Vandenburgh and D. J. Mooney, *Biomaterials*, 2011, **32**, 8905–8914.
3 Y. J. Chuah, Y. Peck, J. E. J. Lau, H. T. Hee and D. A. Wang, *Biomater. Sci.*, 2017, **5**, 613–631.
4 A. Vashist, A. Kaushik, A. Vashist, R. D. Jayant, A. Tomitaka, S. Ahmad, Y. K. Gupta and M. Nair, *Biomater. Sci.*, 2016, **4**, 1535–1554.
5 H. W. Chien, J. Yu, S. T. Li, H. Y. Chen and W. B. Tsai, *Biomater. Sci.*, 2017, **5**, 322–330.
6 O. Chaudhuri, *Biomater. Sci.*, 2017, **5**, 1480–1490.
7 S. Gerecht, J. A. Burdick, L. S. Ferreira, S. A. Townsend, R. Langer and G. Vunjak-Novakovic, *Proc. Natl. Acad. Sci. U. S. A.*, 2007, **104**, 11298–11303.
8 S. K. Hamilton, H. Lu and J. S. Temenoff, *Biomaterials as Stem Cell Niche*, 2010, pp. 119–152.
9 M. P. Lutolf and J. A. Hubbell, *Nat. Biotechnol.*, 2005, **23**, 47–55.
10 M. W. Tibbitt and K. S. Anseth, *Biotechnol. Bioeng.*, 2009, **103**, 655–663.
11 D. S. W. Benoit, M. P. Schwartz, A. R. Durney and K. S. Anseth, *Nat. Mater.*, 2008, **7**, 816–823.
12 R. Langer and D. A. Tirrell, *Nature*, 2004, **428**, 487–492.
13 M. P. Lutolf, P. M. Gilbert and H. M. Blau, *Nature*, 2009, **462**, 433–441.
14 J. Yen, H. Ying, H. Wang, L. Yin, F. Uckun and J. Cheng, *ACS Biomater. Sci. Eng.*, 2016, **2**, 326–335.
15 M. S. Bae, D. H. Yang, J. B. Lee, D. N. Heo, Y. D. Kwon, I. C. Youn, K. Choi, J. H. Hong, G. T. Kim, Y. S. Choi, E. H. Hwang and I. K. Kwon, *Biomaterials*, 2011, **32**, 8161–8171.
16 P. N. Patel, C. K. Smith and C. W. Patrick Jr., *J. Biomed. Mater. Res., Part B*, 2005, **73**, 313–319.
17 K. Y. Lee and D. J. Mooney, *Chem. Rev.*, 2001, **101**, 1869–1879.
18 J. L. Drury and D. J. Mooney, *Biomaterials*, 2003, **24**, 4337–4351.
19 A. Khademhosseini, Y. Ling, J. M. Karp and R. Langer, Micro- and Nanoscale Control of Cellular Environment for Tissue Engineering, in *Nanobiotechnology II: More Concepts and Applications*, ed. C. A. Mirkin and C. M. Niemeyer, Wiley-VCH Verlag GmbH & Co. KGaA, Weinheim, Germany, 2007.
20 J. Zoldan, E. D. Karagiannis, C. Y. Lee, D. G. Anderson, R. Langer and S. Levenberg, *Biomaterials*, 2011, **32**, 9612–9621.
21 K. E. Hammerick, Z. B. Huang, N. Sun, M. T. Lam, F. B. Prinz, J. C. Wu, G. W. Commons and M. T. Longaker, *Tissue Eng., Part A*, 2011, **17**, 495–502.
22 N. D. Leipzig and M. S. Shoichet, *Biomaterials*, 2009, **30**, 6867–6878.
23 O. Chaudhuri, L. Gu, D. Klumpers, M. Darnell, S. A. Bencherif, J. C. Weaver, N. Huebsch, H. P. Lee, E. Lippens, G. N. Duda and D. J. Mooney, *Nat. Mater.*, 2016, **15**, 326.
24 H. Wang and S. C. Heilshorn, *Adv. Mater.*, 2015, **27**, 3717–3736.
25 A. M. Kloxin, M. W. Tibbitt, A. M. Kasko, J. A. Fairbairn and K. S. Anseth, *Adv. Mater.*, 2010, **22**, 61.
26 C. Ninh, M. Cramer and C. J. Bettinger, *Biomater. Sci.*, 2014, **2**, 766–774.
27 Y. Lei and D. V. Schaffer, *Proc. Natl. Acad. Sci. U. S. A.*, 2013, **110**, E5039–E5048.
28 Z. Feng, J. Zhao, Y. Li, S. Xu, J. Zhou, J. Zhang, L. Deng and A. Dong, *Biomater. Sci.*, 2016, **4**, 1493–1502.
29 J. A. Burdick, C. Chung, X. Q. Jia, M. A. Randolph and R. Langer, *Biomacromolecules*, 2005, **6**, 386–391.
30 K. H. Bae and M. Kurisawa, *Biomater. Sci.*, 2016, **4**, 1184–1192.
31 S. Binauld and M. H. Stenzel, *Chem. Commun.*, 2013, **49**, 2082–2102.
32 Y. Zhang, H. Ying, K. R. Hart, Y. Wu, A. J. Hsu, A. M. Coppola, T. A. Kim, K. Yang, N. R. Sottos, S. R. White and J. Cheng, *Adv. Mater.*, 2016, **28**, 7646–7651.
33 H. Ying; and J. Cheng, *J. Am. Chem. Soc.*, 2014, **136**, 16974–16977.
34 H. Ying, Y. Zhang; and J. Cheng, *Nat. Commun.*, 2014, **5**, 3218.

